European Journal of Neuroscience, Vol. 27, pp. 104–113, 2008 doi:10.1111/j.1460-9568.2007.06001.x

Specific inhibitory synapses shift the balance from feedforward to feedback inhibition of hippocampal CA1 pyramidal cells

David Elfant,[1,2] Balázs Zoltán Pál,[1,*] Nigel Emptage[2] and Marco Capogna[1]
[1]MRC Anatomical Neuropharmacology Unit, Mansfield Road, Oxford OX1 3TH, UK
[2]Department of Pharmacology, Mansfield Road, Oxford OX1 3TH, UK

Keywords: hippocampal neurons, interneuron, paired recording, rat, synaptic transmission

Abstract

Feedforward and feedback inhibition are two fundamental modes of operation widespread in the nervous system. We have functionally identified synaptic connections between rat CA1 hippocampal interneurons of the stratum oriens (SO) and interneurons of the stratum lacunosum moleculare (SLM), which can act as feedback and feedforward interneurons, respectively. The unitary inhibitory postsynaptic currents (uIPSCs) detected with K-gluconate-based patch solution at −50 mV had an amplitude of 20.0 ± 2.0 pA, rise time 2.2 ± 0.2 ms, decay time 25 ± 2.2 ms, jitter 1.4 ± 0.2 ms (average ± SEM, $n = 39$), and were abolished by the γ-aminobutyric acid $(GABA)_A$ receptor antagonist 2-(3-carboxypropyl)-3-amino-6-methoxyphenyl-pyridazinium bromide (SR 95531). *Post hoc* anatomical characterization revealed that all but one of the identified presynaptic neurons were oriens-lacunosum moleculare (O-LM) cells, whereas the postsynaptic neurons were highly heterogeneous, including neurogliaform ($n = 4$), basket ($n = 4$), Schaffer collateral-associated ($n = 10$) and perforant path-associated ($n = 9$) cells. We investigated the short-term plasticity expressed at these synapses, and found that stimulation at 10–40 Hz resulted in short-term depression of uIPSCs. This short-term plasticity was determined by presynaptic factors and was not target-cell specific. We found that the feedforward inhibition elicited by the direct cortical input including the perforant path onto CA1 pyramidal cells was modulated through the inhibitory synapses we have characterized. Our data show that the inhibitory synapses between interneurons of the SO and SLM shift the balance between feedback and feedforward inhibition onto CA1 pyramidal neurons.

Introduction

Feedforward and feedback inhibition are widespread in the brain, and one of their major functions is to regulate the timing across different cell populations by controlling the temporal summation of excitatory inputs (Pouille & Scanziani, 2001, 2004). In the hippocampus, CA1 pyramidal cells are under the influence of both these modes of γ-aminobutyric acid (GABA)ergic inhibition. A relevant example of CA1 feedback interneurons is represented by GABAergic interneurons located in the stratum oriens (SO) that are characterized by a horizontal somatodendritic architecture and axons that project to different parts of the somatodendritic domains of pyramidal cells (Maccaferri, 2005; Somogyi & Klausberger, 2005). One class of such interneurons, known as the oriens-lacunosum moleculare (O-LM) cell, receives excitatory postsynaptic potentials (EPSPs) from pyramidal axon collateral branches in the SO (Lacaille *et al.*, 1987; Ali & Thomson, 1998), and in turn innervates the distal dendrites of pyramidal cells in the stratum lacunosum moleculare (SLM) to evoke inhibitory postsynaptic potentials (IPSPs; Maccaferri *et al.*, 2000). The SLM of the CA1 area receives an important excitatory input including the perforant path of the entorhinal cortex (referred to as direct cortical input) in which a feedforward inhibitory circuit is built in. Essentially, the direct cortical input excites CA1 pyramidal cells (Yeckel & Berger, 1990, 1995; Colbert & Levy, 1992), and at the same time activates interneurons in the SLM, which in turn project to CA1 pyramidal cells (Empson & Heinemann, 1995a,b; Remondes & Schuman, 2002). Similar to interneurons of the SO, interneurons of the SLM represent an heterogeneous population of cells, which project to different parts of the somatodendritic domains of pyramidal cells (Lacaille & Schwartzkroin, 1988; Williams & Lacaille, 1992; McBain *et al.*, 1994; Williams *et al.*, 1994; Khazipov *et al.*, 1995; Freund & Buzsaki, 1996; Bertrand & Lacaille, 2001; Maccaferri & Lacaille, 2003; Somogyi & Klausberger, 2005).

During theta oscillatory neuronal activity, O-LM cells fire maximally at the trough of a theta cycle (Klausberger *et al.*, 2003). Conversely, interneurons of the SLM, such as neurogliaform cells (Vida *et al.*, 1998; Price *et al.*, 2005), fire preferentially around the peak of the theta cycle (Fuentealba *et al.*, 2006). Are hippocampal interneurons of the SO and SLM synaptically connected, so that the firing of one type would inhibit the firing of the other? Anatomical data suggest that somatostatin-immunostained boutons of O-LM cells make synaptic contacts with GABAergic profiles in the SLM in addition to their more frequent contacts onto the distal dendrites of pyramidal neurons (Katona *et al.*, 1999). Based on this anatomical information, our aim was to functionally characterize unitary monosynaptic

Correspondence: Dr M. Capogna, as above.
E-mail: marco.capogna@pharm.ox.ac.uk

**Present address*: Department of Physiology, Medical and Health Science Centre, University of Debrecen, PO Box 22, Debrecen, H-4012, Hungary.

Received 2 July 2007, revised 25 October 2007, accepted 15 November 2007

connections between interneurons with the soma in the SO and their interneuron target(s) with the soma in the SLM, and to elucidate which type(s) of postsynaptic interneurons were targeted. In order to understand how these synaptic connections influence the flow of information onto CA1 pyramidal cells, we also investigated their short-term plastic properties and their potential role within the cortical-CA1 circuit.

Materials and methods

Slice preparation

All procedures involving animals were performed using methods approved by the UK Home Office and according to The Animals (Scientific Procedures) Act, 1986. Male postnatal day (P)18–22 Sprague–Dawley rats were anaesthetized with isoflurane, decapitated, and their brain quickly removed and placed into ice-cold high-magnesium artificial cerebrospinal fluid (ACSF; composition in mM: $NaCl_2$, 85; $NaHCO_3$, 25; KCl, 2.5; NaH_2PO_4, 1.25; $CaCl_2$, 0.5; $MgCl_2$, 7; glucose, 10; sucrose, 75) saturated with 95% O_2, 5% CO_2, at pH 7.3. Horizontal sections (300–350 μm; range: from Bregma −6.60 to −4.74) were made consisting of the hippocampus and attached entorhinal cortex, suitable to study preserved entorhinal–hippocampal connection (Witter, 1993). The slices were allowed to recover in recording ACSF [same as above, but (in mM): $NaCl_2$, 130; $CaCl_2$, 2; $MgCl_2$, 2; sucrose, 0] at room temperature for at least 45 min before recording. Interface-type organotypic slice cultures were also prepared by using a standard method (Stoppini *et al.*, 1991). Briefly, male P7 Sprague–Dawley rats were deeply anaesthetized with isoflurane, rapidly decapitated, the brain was dissected out, and the hippocampi were removed and placed into cold minimal essential medium (MEM, Gibco, Paisley, UK). The hippocampi were then sectioned into 400-μm slices and placed on semipermeable membranes (Millicell-CM, Millipore, Watford, UK) in six-well plates containing 1 mL of culture medium consisting of 50% MEM, 25% Hanks balanced salt solution (Gibco), 25% horse serum (Gibco), 1% Pen/Strep (Gibco), 0.003% $NaHCO_3$ (Sigma, Poole, UK), pH 7.3 with Tris. Cultures were incubated at 37 °C with 5% CO_2 for 4 days and at 34 °C with 5% CO_2 for 7–11 days.

Electrophysiology and analysis

Paired whole-cell recordings were performed using an EPC10/3 amplifier (HEKA, Lambrecht, Germany). Acute slices or slice cultures were placed in a recording chamber mounted on the stage of an upright microscope (Axioscope, Zeiss, Germany), superfused with recording ACSF and maintained at a temperature of 33 ± 1 °C. The somata of the interneurons in the SO and SLM of the CA1 area were visually identified based on their shape and size. Borosilicate patch electrodes were filled with (in mM): K-gluconate, 126; HEPES, 10; Na_2Phosphocreatine, 10; KCl, 4; Mg-ATP, 4; Na-GTP, 0.3; biocytin, 0.5%, pH 7.3 with KOH, and had resistances between 4 and 6 MΩ. Access resistance was always monitored to ensure the stability of recording conditions. Cells were only accepted for analysis if the initial series resistance was less than or equal to 35 MΩ and did not change by more than 20% throughout the recording period. The series resistance was 22.2 ± 1.6 MΩ ($n = 35$) and was compensated online by 60–70% in voltage-clamp mode to reduce voltage errors. Presynaptic neurons were voltage-clamped at a holding potential of −60 mV and the postsynaptic neurons were held at −50 mV to enhance the driving force for the Cl^--mediated GABAergic responses. Action currents were elicited in one cell and the corresponding unitary inhibitory postsynaptic current (uIPSC) measured in the postsynaptic neuron. All the drugs were bath-applied and were purchased from Tocris Cookson (Avonmouth, UK).

Minimal extracellular stimulation experiments were conducted in the presence of 20 μM 6,7-dinitroquinoxaline-2,3-dione (DNQX) and 40 μM D-2-amino-5-phosphonopentanoate (D-AP5) by applying rectangular pulses of current (0.4 ms width, intensity range: 30–80 μA) delivered through an isolation unit (A306 Stimulus Isolator, World Precision Instruments, Stevenage, UK) to a monopolar patch pipette filled with ACSF that was placed in the SO. Stimuli were initially applied at higher intensities until a synaptic response could be seen in the postsynaptic cell. Then, the stimulus intensity was gradually reduced until the amplitude of the synaptic response was noticeably smaller, failed at times, and was present in an all-or-none manner (Fig. 1C). In many cases the position of the stimulation electrode was moved to aid in finding the smallest possible amplitude response without generating failures. When extracellular stimulation of the alveus and the direct cortical input was employed, the stimulation of afferents (0.4 ms width; intensity range: 60–200 μA) was obtained using a concentric bipolar electrode (FHC, Bowdoin, ME, USA). In these experiments, the CA3 area was always removed to avoid non-specific activation of pyramidal cells after direct cortical input stimulation and, in some experiments, a cut was performed from the SO to the stratum radiatum (SR) (Dingledine & Langmoen, 1980).

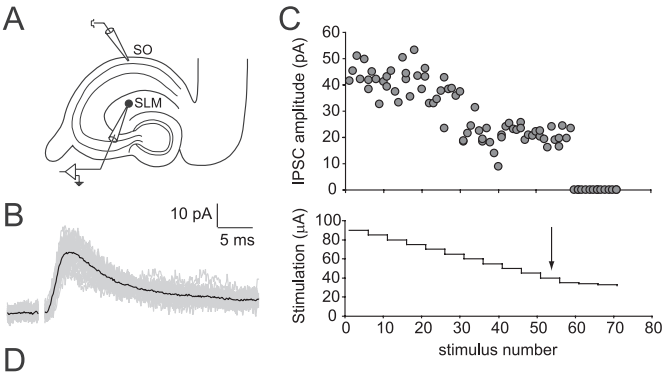

D

Acute Slice

IPSC Parameter	Total	PP	Sch	NG	B	n.d.
Peak Amplitude (pA)	23.3 ± 2.9	25.1 ± 4.0	22.2 ± 8.6	15.8 ± 5.0	26.3 ± 0.6	24.9 ± 5.9
Rise Time (ms)	2.1 ± 0.2	2.0 ± 0.2	2.7 ± 0.5	1.7 ± 0.3	1.6 ± 0.1	1.8 ± 0.4
Decay Tau (ms)	26.1 ± 3.3	30.8 ± 7.6	27.0 ± 9.7	18.7 ± 5.6	20.2 ± 0.6	26.9 ± 4.7
Latency (ms)	3.8 ± 0.2	4.2 ± 0.4	3.1 ± 0.3	4.7 ± 0.4	3.3 ± 0.3	3.8 ± 0.4
Jitter (μs)	1410 ± 248	1056 ± 288	1396 ± 459	1658 ± 999	1557 ± 1234	1578 ± 597
	(n=24)	(n=6)	(n=6)	(n=3)	(n=2)	(n=7)

FIG. 1. Minimal extracellular stimulation in the stratum oriens (SO) of CA1 evokes monosynaptic inhibitory postsynaptic currents (IPSCs) in interneurons of the stratum lacunosum moleculare (SLM). (A) Scheme of the hippocampus depicting the location of the stimulating and recording electrodes in the SO and SLM, respectively. (B) Monosynaptic IPSCs evoked in the presence of glutamate receptor antagonists (20 μM DNQX and 40 μM D-AP5). Individual monosynaptic IPSCs are shown in grey, and the average of 30 traces is shown in black. The stimulation artefact has been removed for clarity. (C) In order to achieve minimal stimulation, the stimulation intensity was gradually decreased (bottom graph) until uIPSCs with constant and smallest amplitude were observed (top graph); further decrease in the stimulation intensity resulted only in failures. The arrow indicates the stimulation intensity used for stimulation of a single fibre in this experiment. (D) Summary of the monosynaptic IPSC parameters evoked by minimal stimulation. All comparisons between different cell types were statistically insignificant ($P > 0.05$ ANOVA). Abbreviations: PP, perforant path-associated interneuron; Sch, Schaffer collateral-associated interneuron; NG, neurogliaform cell; B, basket cell; n.d., not determined.

Data were analysed offline using Patchmaster (HEKA) and Igor Pro 5.05 (Wavemetrics, Lake Oswego, OR, USA). An automated macro was developed in Igor to perform all measurements of synaptic responses including subtraction of traces. Failures were flagged if the IPSCs were of smaller amplitude than three times the standard deviation (SD) of the baseline recording, had a time window smaller than 10 ms or had an onset time that was greater than the average calculated for a file of 30 sweeps plus five times the SD. Synaptic jitter was calculated as the SD of the mean latency. The coefficient of variation (CV = SD/mean) of IPSC peak amplitudes was calculated from 60 sweeps for each experiment. Statistical tests used are indicated throughout the text and were performed using SPSS (Surrey, UK). Values presented in the text and in figures represent the mean ± SEM. The input resistance (R_{in}) was calculated from the slope of a line fitted to the subthreshold range on a plot of the injected current vs the steady-state membrane voltage when a family of hyperpolarizing and depolarizing current injections were applied. The apparent membrane time constant (τ) was calculated by fitting a single exponential to the response of the cell to a current injection of −90 pA in current-clamp mode. Membrane capacitance was calculated as τ/R_{in}. The sag rectification ratio was calculated from the membrane potential at the end of a 0.6 s hyperpolarizing pulse divided by the largest membrane potential change observed in response to a current step of −90 pA. The peak amplitude, afterhyperpolarization and half-width were measured from the initial point of the raising phase of the action potential.

Intracellular labelling and visualization of recorded cells

Following electrophysiological recordings, slices and cultures were immersed overnight in fixative (4% paraformaldehyde, 0.05% glutaraldehyde and 0.2% saturated picric acid in 0.1 M phosphate buffer, pH 7.4). For acute slices, gelatine-embedding and re-sectioning into 60 μm slices was carried out. Recorded cells in the slices were then labelled by avidin-biotinylated horseradish peroxidase complex followed by a peroxidase reaction using diaminobenzidine (0.05%) as the chromogen and H_2O_2 (0.01%) as the substrate. The sections were dehydrated using increasing concentrations of ethanol and permanently mounted on slides. Neurons were drawn (100 × magnification) using a drawing tube attached to a light microscope.

Results

Inhibitory synaptic connections between interneurons of the SO and SLM

Minimal extracellular stimulation of the SO in the presence of ionotropic glutamate receptor antagonists (20 μM DNQX and 40 μM D-AP5) evoked IPSCs in interneurons with the soma located in the SLM, including perforant path- ($n = 6$) and Schaffer collateral-associated ($n = 6$) interneurons, neurogliaform cells ($n = 3$), basket cells ($n = 2$) and cells that were not possible to identify ($n = 7$; Fig. 1). The IPSCs displayed the characteristic properties (amplitude, kinetics, latency and jitter) of a monosynaptic connection (Fig. 1D), and were abolished by the $GABA_A$ receptor antagonist 2-(3-carboxypropyl)-3-amino-6-methoxyphenyl-pyridazinium bromide (SR 95531; 1.2 μM, $n = 4$, not shown). All the synaptic parameters analysed did not statistically differ amongst the interneuronal types (ANOVA, $P > 0.05$).

However, using extracellular stimulation one cannot exclude the recruitment of collaterals from interneurons other than those with their soma in the SO, and the identity of the presynaptic cells remains unknown. To overcome these limitations, we performed paired recordings between cells with the soma located in the SO and cells in the SLM (Fig. 2). In acute slices, we observed monosynaptic uIPSCs in approximately one out of 20 attempts. This low success rate prompted us to perform the same experiment in hippocampal slice cultures of the same age (P18–22), which may display increased connectivity (Debanne *et al.*, 1995). However, we observed no difference in the likelihood to detect synaptically coupled interneurons of SO and SLM in this preparation compared with hippocampal acute slices. The uIPSCs recorded in both preparations showed no difference in peak amplitude, rise time, decay time constant, latency or jitter (Fig. 2E, ANOVA, $P > 0.05$). Likewise, we observed a low number of failures in both acute slices (5 ± 4%) and slice cultures (2 ± 1%, paired *t*-test, $P > 0.05$).

The uIPSCs detected in the paired recording experiments in both preparations had similar properties to the monosynaptic IPSCs evoked by the minimal stimulation protocol (Figs 1D and 2E, ANOVA, $P > 0.05$), except for the latency that was significantly shorter ($P < 0.005$) probably due to the longer delay to elicit firing in the presynaptic cells with the extracellular stimulation technique. Similar to the extracellular stimulation experiments, we recorded uIPSCs in perforant path- ($n = 3$) and Schaffer collateral-associated ($n = 4$) interneurons, a neurogliaform cell ($n = 1$), basket cells ($n = 2$) and non-determined cells ($n = 5$). These were evoked by activation of presynaptic O-LM ($n = 9$), oriens-bistratified (O-Bi; $n = 1$) or unidentified cells ($n = 4$; Fig. 2F). One example of a reconstructed cell pair is illustrated in Fig. 2A. In order to compare the synaptic parameters amongst the different postsynaptic cell types, we pooled the data obtained in acute slices and slice cultures, and observed no significant differences amongst the different cell types (Fig. 2G, ANOVA, $P > 0.05$). When comparing the synaptic parameters in different postsynaptic cells we found no difference between paired recordings and minimal stimulation conditions (unpaired *t*-test, $P > 0.05$). The latency of the extracellular stimulation monosynaptic IPSCs tended to be longer, and this was statistically significant for the perforant path-associated interneurons (unpaired *t*-test, $P < 0.05$).

The uIPSCs were selectively and reversibly blocked by the $GABA_A$ receptor antagonist 1.2 μM SR 95531 ($n = 3$; Fig. 2D). The amplitude and shape of the uIPSCs were independent of the duration of the

FIG. 2. Inhibitory unitary synaptic connections between interneurons of the stratum oriens (SO) and stratum lacunosum moleculare (SLM). (A) Light microscopic reconstruction (× 100) of a biocytin-labelled O-LM neuron (soma and dendrites in black, axon in blue) and a postsynaptic neurogliaform cell (soma and dendrites in red, and axon in blue) in acute slice. Note that the axonal arbour of the O-LM remains segregated within the SLM where it overlaps extensively with the dendritic and axonal arborization of the neurogliaform cell; PYR, stratum pyramidale. (B) Scheme of the hippocampus depicting the location of the presynaptic (black) and postsynaptic (red) recorded neurons. (C) Electrophysiology of the cell pair illustrated in (A). The upper trace shows an action current elicited in the O-LM cell (black) and the lower trace illustrates the resulting unitary inhibitory postsynaptic currents (uIPSCs) in the neurogliaform cell (average in red, 30 individual sweeps in grey). (D) The uIPSCs were entirely mediated by $GABA_A$ receptors. Time course of the reversible effect of 1.2 μM 2-(3-carboxypropyl)-3-amino-6-methoxyphenyl-pyridazinium bromide (SR 95531) on the amplitude of the uIPSC. (E) Summary of the properties of the uIPSCs in the paired recording experiments performed in acute slices and slice cultures. All comparisons between acute slices and slice cultures were statistically insignificant ($P > 0.05$ ANOVA). (F) Frequency histograms of the occurrence of different types of postsynaptic recorded interneurons. Presynaptic cells in the paired recording experiments were O-LM (black bars), O-Bi (grey bar) or not determined (white bars). (G) Summary of the properties of the uIPSCs pooled from paired recording experiments performed in acute slices and slice cultures for each postsynaptic cell type. All comparisons amongst cell types were statistically insignificant ($P > 0.05$ ANOVA). Abbreviations in (F) and (G): PP, perforant path-associated interneuron; Sch, Schaffer collateral-associated interneuron; NG, neurogliaform cell; B, basket cell; n.d., not determined.

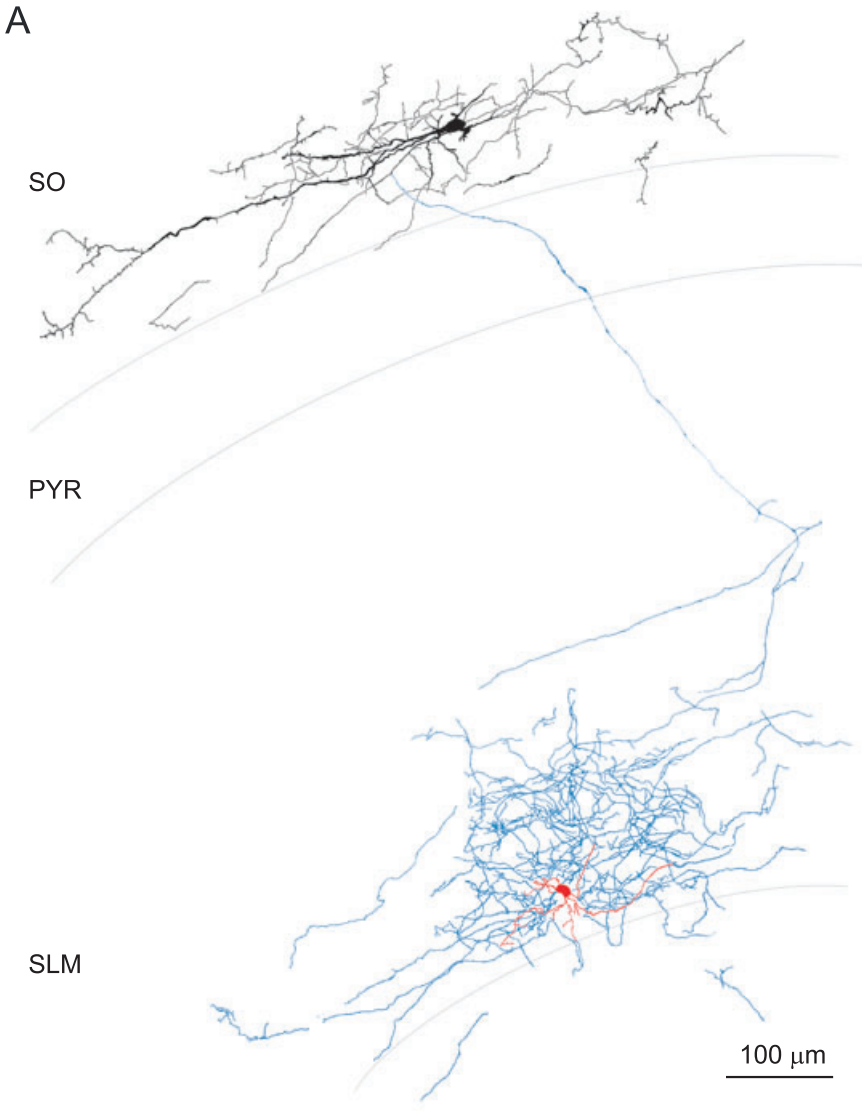

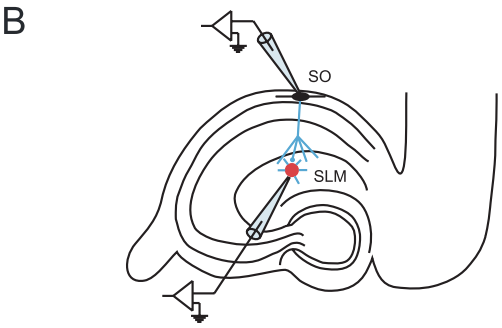

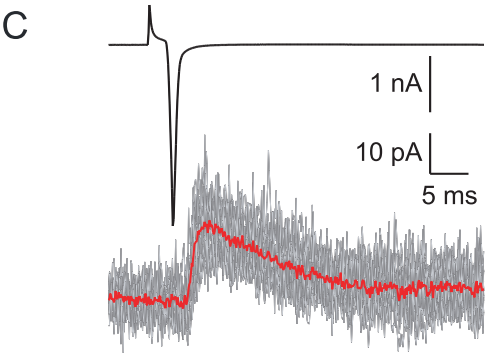

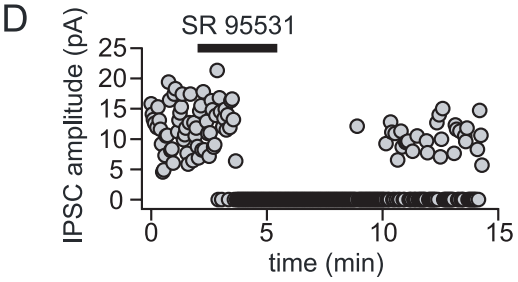

E

	Acute Slice	*Slice Culture*
IPSC Parameter	**Mean ± SEM**	**Mean ± SEM**
Peak Amplitude (pA)	15.3 ± 2.0	14.5 ± 3.1
Rise Time (ms)	2.3 ± 0.6	2.7 ± 0.6
Decay Tau (ms)	23.0 ± 4.9	23.7 ± 2.5
Latency (ms)	2.3 ± 0.1	2.4 ± 0.3
Jitter (μs)	1187 ± 124	1796 ± 236
	(n=7)	(n=8)

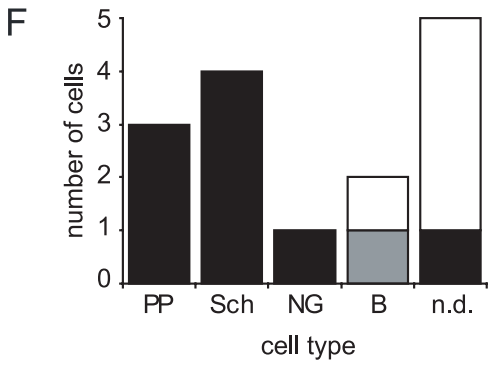

G

Acute Slice and Slice Culture					
IPSC Parameter	**PP**	**Sch**	**NG**	**B**	**n.d.**
Peak Amplitude (pA)	15.3 ± 0.6	19.5 ± 4.7	19.2	11.7 ± 1.0	11.4 ± 3.6
Rise Time (ms)	1.7 ± 0.2	1.9 ± 0.4	2.2	2.6 ± 1.3	3.2 ± 1.1
Decay Tau (ms)	26.2 ± 1.3	31.2 ± 4.5	10.8	16.5 ± 3.9	20.7 ± 5.0
Latency (ms)	2.2 ± 0.1	2.4 ± 0.5	2.3	1.6 ± 0.1	2.7 ± 0.3
Jitter (μs)	1784 ± 499	1291 ± 202	1602	1467 ± 557	1525 ± 325
	(n=3)	(n=4)	(n=1)	(n=2)	(n=5)

voltage pulse applied to the presynaptic cell (not shown), indicating that changes in the somatic membrane potential of the presynaptic cell were not electrotonically conducted to the nerve terminal (Alle & Geiger, 2006), but rather that neurotransmitter release was triggered by action potentials actively propagated along the axon (Poncer *et al.*, 1997).

Anatomical identity of the recorded interneurons

All the recorded neurons were filled with biocytin, and in 69% of the cases their identity was successfully determined based on soma location, size, and dendritic and axonal arborization patterns. As delineated above, in both paired recordings and minimal stimulation, we recorded IPSCs from various postsynaptic cell types. Our classification was mainly based on the axonal distribution pattern of the recorded cells. In brief, neurogliaform neurons were characterized by a round cell body and short, non-spiny dendrites arranged in a stellate pattern around the cell body, and by an extremely dense axonal arbour arranged close to the soma, which was the hallmark of this cell type (Fig. 2A). Perforant path-associated interneurons mainly innervated the SLM of the CA1 area, but had also collaterals innervating other hippocampal layers as well as the dentate gyrus, and their dendrites were usually contained within the SR and SLM. Schaffer collateral-associated interneurons had axonal arbours that were mainly located in the SR, but collaterals were often found in other layers of the hippocampus, their dendritic tree had a stellate appearance, and was confined to the SR and SLM. Finally, basket cells had a dense terminal axonal arbour within the pyramidal cell layer, and their dendritic arbours were radially elongated throughout all hippocampal layers. These observations are consistent with the heterogeneity of interneurons previously described in the SLM (Vida *et al.*, 1998). Furthermore, the interneurons exhibited various firing patterns in response to depolarizing current pulses. Representative examples are shown in Fig. 3. Specifically, O-LM cells were characterized by a large, fast spike afterhyperpolarization, and also a pronounced 'sag' in response to hyperpolarizing current injections (Ali & Thomson, 1998). Neurogliaform cells displayed a delayed action potential (Price *et al.*, 2005), whereas Schaffer collateral-associated, perforant path-associated and basket cells exhibited variable accommodating firing patterns (Vida *et al.*, 1998).

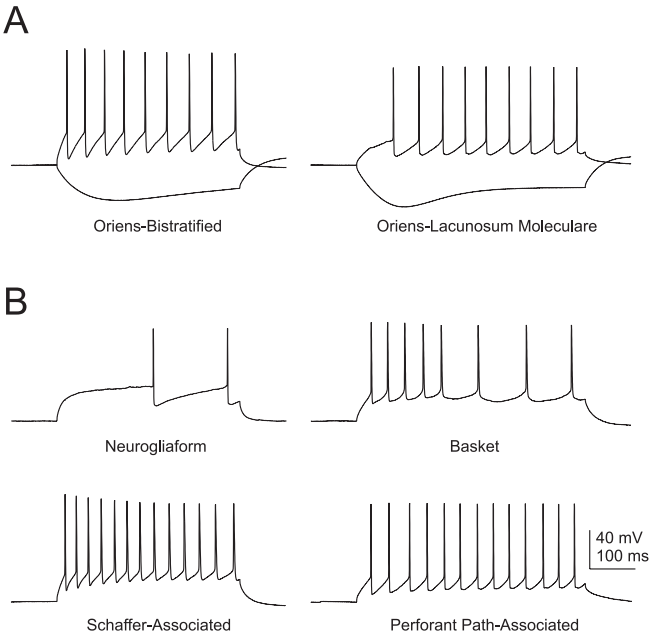

C

	O-LM	O-Bi	PP	Sch	B	NG
Resting Membrane Potential (mV)	-65.0	-77.8	-62.0	-61.1	-60.0	-65.9
Input Resistance (MΩ)	282.6	232.2	321.3	644.1	449.2	318.2
Membrane time constant (ms)	31.1	50.2	39.5	47.0	47.8	14.9
Membrane Capacitance (nF)	0.11	0.22	0.12	0.07	0.11	0.05
Sag Rectification Ratio	0.53	0.67	0.87	0.91	0.97	0.99
Spike Half Width (ms)	1.1	1.0	0.8	1.1	1.4	0.8
Spike Peak Amplitude (mV)	83.5	91.4	71.7	83.7	72.8	59.9
Fast After-Hyperpolarisation (mV)	18.1	25.0	18.8	17.6	16.6	19.5

FIG. 3. Firing patterns and intrinsic membrane properties of the recorded neurons. (A) Presynaptic neurons. Firing patterns and characteristic 'sag' of representative O-LM and O-Bi interneurons in response to a depolarizing (100 pA) and hyperpolarizing current pulse (−90 pA). (B) Postsynaptic neurons. Firing patterns of interneurons of the SLM elicited by a depolarizing current pulse (100 pA). All the recorded neurons were anatomically identified off line. (C) Table showing the values of some intrinsic membrane responses for each cell shown. Abbreviations: O-LM, oriens-lacunosum moleculare cell; O-Bi, oriens-bistratified cell; PP, perforant path-associated interneuron; Sch, Schaffer collateral-associated interneuron; B, basket cell; NG, neurogliaform cell.

Short-term plasticity of the SO–SLM interneuron synapses

In vivo, entorhinal–hippocampal circuits display activity at theta (10 Hz) and gamma (40 Hz) frequency ranges (Chrobak *et al.*, 2000). Therefore, to explore the dynamic properties of the synaptic connections observed, we used different stimulation frequencies within this range. Data from minimal stimulation ($n = 17$), paired recordings in acute slices ($n = 5$) and in slice cultures ($n = 4$) were pooled because they showed similar phenotypes. Two stimuli with intervals of 25, 50 and 100 ms elicited paired-pulse depression (PPD) in all cells tested ($n = 26$; Fig. 4A). To verify whether PPD was elicited by pre- or postsynaptic factors, a CV analysis of PPD was performed assuming a simple binomial mode of release (Malinow & Tsien, 1990; Bartos *et al.*, 2001). The inverse of the square of the CV for the second IPSC was plotted against the mean; both were normalized to the respective values of the first IPSC. Most data points were located below the identity line, suggesting that PPD was caused mainly by presynaptic factors ($R^2 = 0.438$; Fig. 4B). The PPD was not dependent on the anatomical identity of the postsynaptic cells (ANOVA, $P > 0.05$; Fig. 4C). Likewise, 10 stimuli at 10 Hz or 40 Hz evoked IPSCs that exhibited short-term depression in both minimal stimulation and paired recording experiments (Fig. 4D). A train of stimuli at 40 Hz elicited a significantly stronger depression than at 10 Hz (unpaired *t*-test, $P < 0.005$; Fig. 4E).

The activation of synapses between interneurons of SO and SLM favours feedback versus feedforward inhibition of CA1 pyramidal cells

The interneurons of the SLM that are targeted by the inhibitory synapses characterized in this study are also monosynaptically excited by the direct cortical input and in turn provide feedforward inhibition onto the distal dendrites of pyramidal neurons (Colbert & Levy, 1992; Williams *et al.*, 1994). Therefore, we hypothesized that activation of feedback interneurons of the SO would shift the balance from feedforward to feedback inhibition of CA1 pyramidal cells by inhibiting the interneurons of the SLM. To test this possibility we studied the effect of a conditioning short train of stimuli applied to the alveus (S1) on the feedforward inhibition mediated by the activation of

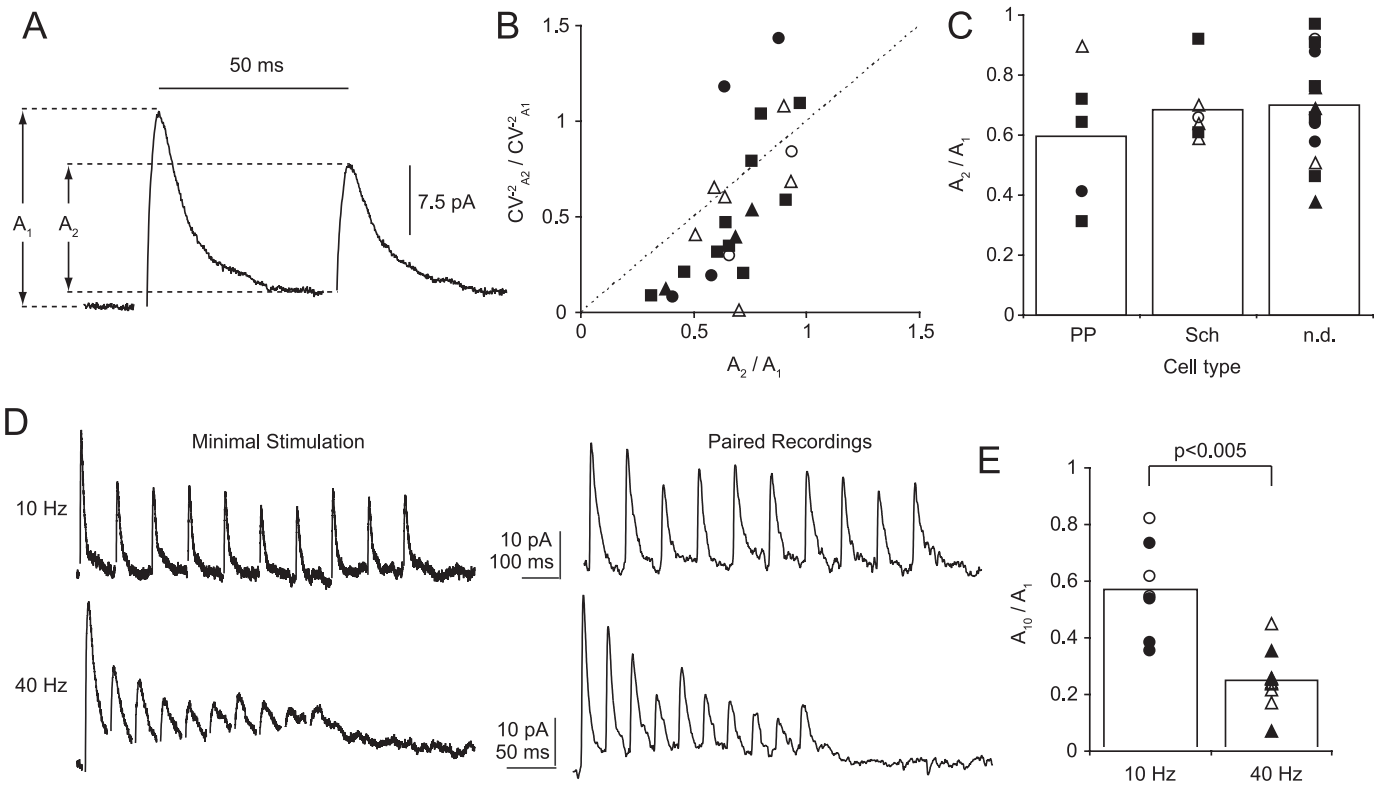

FIG. 4. Dynamics of transmission at inhibitory SO–SLM synapses. (A) IPSCs were evoked by two action potentials in the presynaptic cell or by extracellular stimulation and resulted in PPD. The IPSCs shown are averages from 30 single traces evoked by minimal stimulation with the stimulus artefact removed for clarity. A_1 and A_2 were measured from the preceding baseline. (B) The inverse of the square of the coefficient of variation (CV^{-2}) of the second IPSC (A_2) divided by the CV^{-2} of the first IPSC (A_1) was plotted against the mean peak amplitude of the second IPSC (A_2) divided by the mean peak amplitude of the first IPSC (A_1). Note that most of the data points fall below the unitary line, indicating a presynaptic mechanism of short-term depression. (C) Postsynaptic cell type did not determine the mean PPD value; the mean PPD value of all experiments was 0.67. The comparison between the values in PP, Sch and n.d. cells was not statistically significant ($P > 0.05$ ANOVA). Abbreviations: PP, perforant path-associated interneuron; Sch, Schaffer collateral-associated interneuron; n.d., not determined. (D) The uIPSCs depressed when challenged with a train of 10 stimuli at a frequency of 10 Hz (upper trace) and 40 Hz (bottom trace) in both minimal stimulation experiments (left) or paired recordings (right). Each trace is an average of 10 sweeps; the stimulation artefacts (left) or presynaptic action currents (right) are not shown for clarity. (E) Quantification of short-term depression as peak amplitude of the 10th IPSC (A_{10}) divided by the first IPSC (A_1) of the train. The 40-Hz stimulation elicited stronger synaptic depression than 10 Hz ($P < 0.005$, unpaired t-test). Note in (B), (C) and (E), filled symbols refer to minimal stimulation protocol and white symbols to pair recording experiments; triangles refer to an ISI of 25 ms, squares 50 ms, circles 100 ms.

the interneurons of the SLM by the direct cortical input (S2) recorded intracellularly in CA1 pyramidal neurons. This protocol was only performed in acute slices. The placement of the extracellular electrodes in the slice and a simplified scheme of the synaptic circuit involved are illustrated in Fig. 5A and B. The delivery of S1 in the alveus, which contains the recurrent axon collaterals of CA1 pyramidal cells, elicited feedback IPSPs (Fig. 5C) that were abolished by 3 μM SR 95531 alone ($n = 5$, not shown) or together with the $GABA_B$ receptor antagonist 5 μM (2S)-3-[[(1S)-1-(3,4-dichlorophenyl)ethyl]amino-2-hydroxypropyl](phenylmethyl)phosphinic acid (CGP 55845; $n = 1$, not shown), and in all cases were abolished by 20 μM DNQX and 40 μM D-AP5 ($n = 13$, not shown). We used trains of three stimuli at 100 Hz, which have a higher probability to monosynaptically evoke action potentials in O-LM neurons than one stimulus (Pouille & Scanziani, 2004). On the other hand, S2 elicited an EPSP followed by an early IPSP, and in some cells a clearly detectable late IPSP (Fig. 5D). These synaptic potentials were also virtually abolished by DNQX and D-AP5 ($n = 13$, not shown). The EPSP was enhanced in amplitude and duration, and the early IPSP was blocked by the $GABA_A$ receptor antagonist SR 95531 (not shown, $n = 6$), and the late IPSP was abolished by CGP 55845 ($n = 5$; Fig. 5D), consistent with previous observations (Empson & Heinemann, 1995b). These results are consistent with the activation of local feedforward interneurons. Next, when we paired S1 (conditioning stimulus) with S2 (test stimulus) at interstimulus intervals (ISI) ranging from 7 to 57 ms, all the synaptic potentials were reduced (Fig. 5E). Crucially, when the responses evoked by S1 were subtracted from traces evoked by S1S2, the EPSP size was unchanged as compared with control traces elicited by S2 alone ($n = 11$, paired t-test, $P > 0.05$), whereas the IPSPs were still reduced as compared with control traces evoked by S2 (paired t-test, $P < 0.005$ early IPSP, $n = 11$; $P < 0.05$ late IPSP, $n = 4$, for ISI = 57 ms; Fig. 5F). The subtraction effectively removes direct feedback inhibition onto CA1 pyramids and eliminates any overlapping between the synaptic potentials elicited by S1 and S2, thus the reduction of the IPSPs must be due to inhibition of the feedforward interneurons. After the pairing protocol, S2 alone elicited IPSPs with values similar to controls (Fig. 5G), showing reversibility and absence of any long-term effect. On average, the early and late IPSPs evoked by S2 were -1.4 ± 0.3 mV and -1.9 ± 0.5 mV in control, -0.9 ± 0.2 mV and -1.5 ± 0.4 mV when S1 was elicited 57 ms before S2, and -1.2 ± 0.2 mV and -2 ± 0.1 mV after S2 only again. Furthermore, the EPSP evoked by S2 was 1.9 ± 0.3 mV, 2 ± 0.4 mV when S1 was elicited 57 ms before S2, and 2.1 ± 0.3 mV after S2 only again.

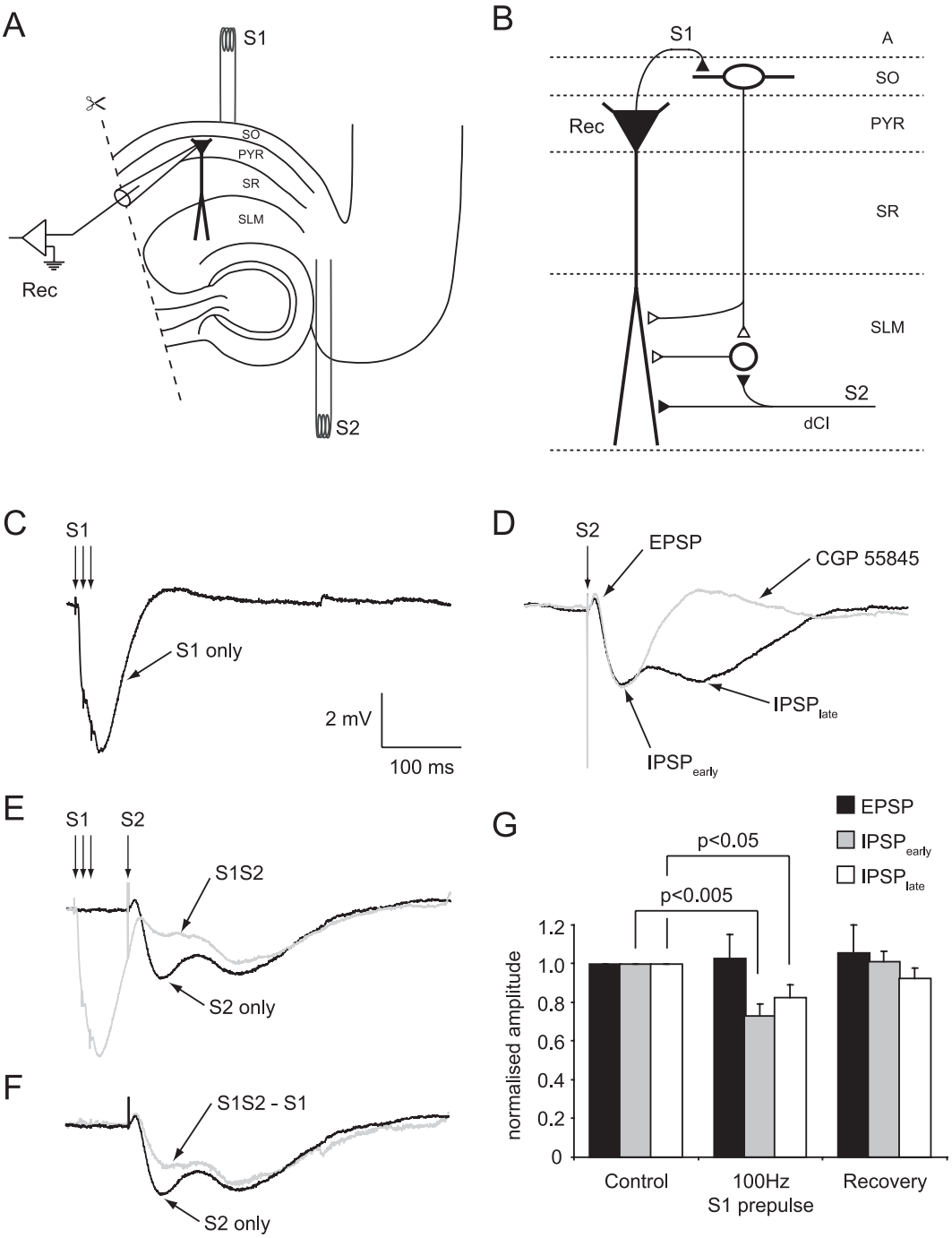

FIG. 5. Inhibitory synapses between interneurons of stratum oriens (SO) and stratum lacunosum moleculare (SLM) contribute to change the balance from feedforward to feedback inhibition of CA1 pyramidal cells. (A) Scheme of hippocampus and placement of the stimulating (S1, S2) and recording (Rec) extracellular electrodes in the slice. The dashed lines indicate cuts made in the slices before recording. (B) Simplified scheme of the hypothetical role of the synapses between interneurons of SO and SLM in the entorhinal–CA1 hippocampal circuit. Filled symbols depict the excitatory cell and synapses, open symbols illustrate inhibitory cells and synapses; A, Alveus; dCI, direct cortical input; PYR, stratum pyramidale; SR, stratum radiatum. (C) Extracellular stimulation in S1 (three pulses, 100 Hz) evoked feedback inhibitory postsynaptic potentials (IPSPs) in a CA1 pyramidal cell. (D) Single extracellular stimulation in S2 elicited a sequence of an excitatory postsynaptic potential (EPSP) followed by feedforward early and late IPSPs. The late IPSP was abolished by 5 μM (2S)-3-[[(1S)-1-(3,4-dichlorophenyl)ethyl]amino-2-hydroxypropyl](phenylmethyl)phosphinic acid (CGP 55845). (E) Superimposed traces showing the response after S2 alone (black trace) and when S2 was preceded by a conditioning stimulation in S1 elicited 57 ms before S2 (grey trace). Note that the conditioning stimulation decreased all the synaptic potentials evoked by S2. (F) Superimposed traces illustrating the response after S2 alone (black trace) and when the S1 traces were subtracted from S1S2 traces (grey trace). Note that the EPSPs were similar in the two traces, whereas the IPSPs were reduced after stimulation of S1. All traces shown are averages of 10 sweeps from the same cell, the synaptic potentials were evoked at the resting membrane potential of −64 mV. (G) Pooled data showing the normalized peak amplitude of EPSP ($n = 11$), early and late IPSPs ($n = 11$ and 4, respectively), evoked by S2 (control), S2 preceded by S1 (ISI = 57 ms; 100 Hz S1 prepulse), S2 alone again (recovery). The amplitudes are measured after the subtraction of the IPSP evoked by S1. The raw data were statistically compared by a paired *t*-test and the significant comparisons are highlighted.

Histograms showing pooled normalized data are illustrated in Fig. 5G. Thus, interneurons of SLM are inhibited by interneurons of SO contributing to a shift from feedforward to feedback inhibition of hippocampal CA1 pyramidal cells.

Discussion

Inhibitory synaptic connections between interneurons of the SO and SLM

In this work we functionally characterize the monosynaptic connections between interneurons with the soma in the SO and SLM of the CA1 hippocampus. Most of the identified presynaptic neurons were O-LM cells making connections with a heterogeneous population of postsynaptic interneurons including neurogliaform cells, perforant path-associated interneurons, Schaffer collateral-associated interneurons and basket cells. Thus, we provide a functional demonstration of the finding by electron microscopy that about 8% of the targets of somatostatin-positive O-LM terminals in the SLM are GABAergic profiles (Katona *et al.*, 1999). Likewise, previous anatomical work described that in the hippocampal dentate gyrus, hilar-perforant path-associated cells, which resemble O-LM cells, innervate parvalbumin-immunoreactive interneurons (Sik *et al.*, 1997). Our results are also consistent with a previous report that shows the presence of IPSCs in interneurons of SLM upon non-minimal bulk extracellular stimulation in the SO (Khazipov *et al.*, 1995).

Using extracellular stimulation, one cannot exclude the recruitment of collaterals from interneurons other than those with their soma in the SO, such as vasoactive intestinal polypeptide-containing interneurons that specifically contact other interneurons (Acsady *et al.*, 1996). For this reason, we have also used paired recordings and found that both approaches resulted in IPSCs with similar amplitude, kinetic parameters and short-term plasticity. Furthermore, the IPSCs obtained by both techniques were recorded from a similar pattern of postsynaptic cell types. This suggests that in our experiments the extracellular stimulation recruited inhibitory fibres originating from the same types of presynaptic cells as those recorded from paired recordings. Interestingly, the likelihood to detect monosynaptically connected interneurons, and the properties and kinetic parameters of the uIPSCs were similar in hippocampal acute slices compared with slice cultures. Therefore, this inhibitory synaptic connection appears to be insensitive to circuit reorganization leading to increased synaptic connectivity, which has been documented in some cases in the slice culture preparation (Zimmer & Gahwiler, 1984; Thomas *et al.*, 2005).

The SO contains the somata of several different interneuronal types, which project toward different and specific postsynaptic domains of the CA1 pyramidal cell (Maccaferri, 2005). The somatodendritic location of these interneurons in the SO is ideal to receive recurrent axon collateral branches from pyramidal cells (Lacaille *et al.*, 1987; Ali & Thomson, 1998), in addition to projections from the direct cortical input and Schaffer collaterals (Maccaferri & McBain, 1995). In turn, these interneurons act as feedback regulators by eliciting inhibitory unitary events in pyramidal cells (Blasco-Ibanez & Freund, 1995; Maccaferri & McBain, 1995; Maccaferri *et al.*, 2000; Pouille & Scanziani, 2004). In particular, the O-LM cell that innervates the distal dendrites of pyramidal cells evokes uIPSCs with smaller amplitude and slower kinetics than those evoked by perisomatically targeting interneurons such as basket cells (Maccaferri *et al.*, 2000). Conversely, cells with the soma in the SLM act as feedforward inhibitory interneurons when activated by the direct cortical input perforant path (Empson & Heinemann, 1995b,a; Remondes & Schuman, 2002), although because their dendrites often span several layers (e.g. parvalbumin- and cholecystokinin-containing basket cells) different excitatory inputs can also recruit them in feedback circuits (Vida *et al.*, 1998). Interneurons of the SLM project to pyramidal cells (Vida *et al.*, 1998), but also make an extensive network via electrical and chemical connections (Williams *et al.*, 1994; Price *et al.*, 2005; Zsiros & Maccaferri, 2005; Zsiros *et al.*, 2007). Furthermore, cells of SLM exist, such as vasoactive intestinal polypeptide-containing interneurons, which selectively contact other GABAergic cells (Acsady *et al.*, 1996).

The short-term plastic properties of synapses between O-LM cells and interneurons of the SLM differ from the ones previously reported between O-LM and CA1 pyramidal cells (Maccaferri *et al.*, 2000). Specifically, a train of action potentials in O-LM cells evokes a clear-cut synaptic depression in the interneurons of the SLM, whereas a similar train elicits a steady response in CA1 pyramidal cells. Thus, the dynamic properties of the O-LM cells output are target specific, and these are likely to tune the overall inhibition impinging upon CA1 pyramidal cells.

Functional consequences

How do the inhibitory connections between interneurons of the SO and SLM influence the CA1 network? The synaptic connections characterized in this study are most likely located in the SLM of the CA1 area in which pyramidal cells receive excitatory input from the entorhinal cortex via the direct cortical input (Witter *et al.*, 1988). We reasoned that it is therefore likely that the monosynaptic connections characterized in the present work also have a modulatory action on the direct cortical input providing a direct link between CA1 feedback and feedforward inhibitory interneurons. The direct cortical input elicits firing in CA1 pyramidal cells, especially when Schaffer collaterals are quasi-simultaneously active (Jarsky *et al.*, 2005). At high firing frequencies (25–100 Hz), pyramidal cells preferentially recruit interneurons in the SO (Pouille & Scanziani, 2004) that, in turn, send feedback inhibition to the distal dendrites of pyramids (Maccaferri *et al.*, 2000), but also, as we describe here, inhibit interneurons of the SLM. In this way, the distal dendrites of pyramidal cells are under two inhibitory influences: feedback and feedforward inhibition (Dvorak-Carbone & Schuman, 1999; Price *et al.*, 2005). Our data suggest a functional role of these inhibitory synapses in the regulation of the balance between feedforward and feedback inhibition. This type of modulation is likely to be highly dynamic because of the short-term plastic properties of O-LM neurons. Specifically, these neurons are synaptically recruited by pyramidal cells only after several stimuli in a train (Pouille & Scanziani, 2004). On the other hand, the synapses between O-LM cells and interneurons of SLM display short-term depression, as we documented here. Thus, the prominence of feedback or feedforward circuits dynamically changes to determine the degree of inhibition of the direct cortical input excitation of pyramidal cell dendrites. However, the shift in the balance between feedforward and feedback inhibition may also be controlled by other mechanisms in addition to the synaptic connection we have described. For instance, the GABA released by feedback inhibition may activate $GABA_B$ receptors located at the axon terminal of interneurons of the SLM (Price *et al.*, 2005) and reduce direct cortical input-mediated IPSPs. It is also important to keep in mind that the same interneurons could participate in both feedforward and feedback inhibition, such as parvalbumin- and cholecystokinin-containing basket cells and axo-axonic cells (Vida *et al.*, 1998; Somogyi & Klausberger, 2005). Thus, short-term synaptic plasticity affecting these interneurons could also contribute to the decreased inhibitory responses described in Fig. 5. The smaller decrease in the $GABA_B$ receptor-mediated response may reflect that

inhibition of the CA1 pyramidal cell dendrites containing high levels of $GABA_B$ receptors mediated by dendritic targeting interneurons is less affected than inhibition to the soma mediated by basket cells. Finally, our extracellular stimulations may also activate several types of interneuron with the soma in any hippocampal layer and contribute to the observed shift. Our data agree with a previous report showing that long-term depression in the CA3–CA1 Schaffer collateral pathway is propagated to interneurons in the SO leading to disinhibition of the direct cortical input (Maccaferri & McBain, 1995). We suggest that the monosynaptic connection uncovered in the present study provides a substrate for the finding that O-LM cells are recruited at the trough of a theta cycle whereas neurogliaform cells in the SLM fire around the peak of the cycle (Klausberger *et al.*, 2003; Fuentealba *et al.*, 2006). The inhibition of interneurons of SLM by those of SO could also contribute to the phase shift of theta oscillations observed from SLM to SO (Bragin *et al.*, 1995).

Conclusions

Interneurons with the soma in the SO provide monosynaptic inhibitory events not only to pyramidal neurons (Maccaferri *et al.*, 2000) but also to other interneurons of the SLM. We propose that these inhibitory synapses can change the balance between feedforward and feedback inhibition of CA1 pyramidal cells in the synaptic dialogue between the entorhinal cortex and the hippocampus.

Acknowledgements

This work was supported by the Medical Research Council (UK). We thank Professor Peter Somogyi and Professor Dmitri Rusakov, Drs Kirill Volynski, Raffaella Geracitano, Theofanis Karayannis and Miss Tatjana Lalic for their comments on the data and/or a previous version of the manuscript. We also thank Romana Hauer and Ben Micklem for their technical help.

Abbreviations

ACSF, artificial cerebrospinal fluid; CGP 55845, (2S)-3-[[(1S)-1-(3,4-dichlorophenyl)ethyl]amino-2-hydroxypropyl](phenylmethyl)phosphinic acid; CV, coefficient of variation; D-AP5, D-2-amino-5-phosphonopentanoate; DNQX, 6,7-dinitroquinoxaline-2,3-dione; EPSP, excitatory postsynaptic potential; GABA, γ-aminobutyric acid; IPSC, inhibitory postsynaptic current; IPSP, inhibitory postsynaptic potential; ISI, interstimulus interval; MEM, minimum essential medium; O-Bi, oriens-bistratified cell; O-LM, oriens-lacunosum moleculare cell; P, postnatal day; PPD, paired-pulse depression; SD, standard deviation; SEM, standard error of the mean; SLM, stratum lacunosum moleculare; SO, stratum oriens; SR, stratum radiatum; SR 95531, 2-(3-carboxypropyl)-3-amino-6-methoxyphenyl-pyridazinium bromide; uIPSCs, unitary inhibitory postsynaptic currents.

References

Acsady, L., Gorcs, T.J. & Freund, T.F. (1996) Different populations of vasoactive intestinal polypeptide-immunoreactive interneurons are specialized to control pyramidal cells or interneurons in the hippocampus. *Neuroscience*, **73**, 317–334.

Ali, A.B. & Thomson, A.M. (1998) Facilitating pyramid to horizontal oriens-alveus interneurone inputs: dual intracellular recordings in slices of rat hippocampus. *J. Physiol.*, **507**, 185–199.

Alle, H. & Geiger, J.R. (2006) Combined analog and action potential coding in hippocampal mossy fibers. *Science*, **311**, 1290–1293.

Bartos, M., Vida, I., Frotscher, M., Geiger, J.R. & Jonas, P. (2001) Rapid signaling at inhibitory synapses in a dentate gyrus interneuron network. *J. Neurosci.*, **21**, 2687–2698.

Bertrand, S. & Lacaille, J.C. (2001) Unitary synaptic currents between lacunosum-moleculare interneurones and pyramidal cells in rat hippocampus. *J. Physiol.*, **532**, 369–384.

Blasco-Ibanez, J.M. & Freund, T.F. (1995) Synaptic input of horizontal interneurons in stratum oriens of the hippocampal CA1 subfield: structural basis of feed-back activation. *Eur. J. Neurosci.*, **7**, 2170–2180.

Bragin, A., Jando, G., Nadasdy, Z., Hetke, J., Wise, K. & Buzsaki, G. (1995) Gamma (40–100 Hz) oscillation in the hippocampus of the behaving rat. *J. Neurosci.*, **15**, 47–60.

Chrobak, J.J., Lorincz, A. & Buzsaki, G. (2000) Physiological patterns in the hippocampo-entorhinal cortex system. *Hippocampus*, **10**, 457–465.

Colbert, C.M. & Levy, W.B. (1992) Electrophysiological and pharmacological characterization of perforant path synapses in CA1: mediation by glutamate receptors. *J. Neurophysiol.*, **68**, 1–8.

Debanne, D., Guerineau, N.C., Gähwiler, B.H. & Thompson, S.M. (1995) Physiology and pharmacology of unitary synaptic connections between pairs of cells in areas CA3 and CA1 of rat hippocampal slice cultures. *J. Neurophysiol.*, **73**, 1282–1294.

Dingledine, R. & Langmoen, I.A. (1980) Conductance changes and inhibitory actions of hippocampal recurrent IPSPs. *Brain Res.*, **185**, 277–287.

Dvorak-Carbone, H. & Schuman, E.M. (1999) Patterned activity in stratum lacunosum moleculare inhibits CA1 pyramidal neuron firing. *J. Neurophysiol.*, **82**, 3213–3222.

Empson, R.M. & Heinemann, U. (1995a) Perforant path connections to area CA1 are predominantly inhibitory in the rat hippocampal-entorhinal cortex combined slice preparation. *Hippocampus*, **5**, 104–107.

Empson, R.M. & Heinemann, U. (1995b) The perforant path projection to hippocampal area CA1 in the rat hippocampal-entorhinal cortex combined slice. *J. Physiol.*, **484**, 707–720.

Freund, T.F. & Buzsaki, G. (1996) Interneurons of the hippocampus. *Hippocampus*, **6**, 347–470.

Fuentealba, P., Klausberger, T., Karayannis, T., Huck, J., Suen, W., Studer, M., Capogna, M. & Somogyi, P. (2006) Firing pattern and synaptic targets of GABAergic neurogliaform cells in the hippocampus in vivo. In *Proceedings of the 5th Forum of European Neuroscience*, Vienna, Austria, 8–12 July 2006, p. 178.

Jarsky, T., Roxin, A., Kath, W.L. & Spruston, N. (2005) Conditional dendritic spike propagation following distal synaptic activation of hippocampal CA1 pyramidal neurons. *Nat. Neurosci.*, **8**, 1667–1676.

Katona, I., Acsady, L. & Freund, T.F. (1999) Postsynaptic targets of somatostatin-immunoreactive interneurons in the rat hippocampus. *Neuroscience*, **88**, 37–55.

Khazipov, R., Congar, P. & Ben-Ari, Y. (1995) Hippocampal CA1 lacunosum-moleculare interneurons: modulation of monosynaptic GABAergic IPSCs by presynaptic GABAB receptors. *J. Neurophysiol.*, **74**, 2126–2137.

Klausberger, T., Magill, P.J., Marton, L.F., Roberts, J.D., Cobden, P.M., Buzsaki, G. & Somogyi, P. (2003) Brain-state- and cell-type-specific firing of hippocampal interneurons in vivo. *Nature*, **421**, 844–848.

Lacaille, J.C., Mueller, A.L., Kunkel, D.D. & Schwartzkroin, P.A. (1987) Local circuit interactions between oriens/alveus interneurons and CA1 pyramidal cells in hippocampal slices: electrophysiology and morphology. *J. Neurosci.*, **7**, 1979–1993.

Lacaille, J.C. & Schwartzkroin, P.A. (1988) Stratum lacunosum-moleculare interneurons of hippocampal CA1 region. I. Intracellular response characteristics, synaptic responses, and morphology. *J. Neurosci.*, **8**, 1400–1410.

Maccaferri, G. (2005) Stratum oriens horizontal interneurone diversity and hippocampal network dynamics. *J. Physiol.*, **562**, 73–80.

Maccaferri, G. & Lacaille, J.C. (2003) Interneuron diversity series: hippocampal interneuron classifications – making things as simple as possible, not simpler. *Trends Neurosci.*, **26**, 564–571.

Maccaferri, G. & McBain, C.J. (1995) Passive propagation of LTD to stratum oriens-alveus inhibitory neurons modulates the temporoammonic input to the hippocampal CA1 region. *Neuron*, **15**, 137–145.

Maccaferri, G., Roberts, J.D., Szucs, P., Cottingham, C.A. & Somogyi, P. (2000) Cell surface domain specific postsynaptic currents evoked by identified GABAergic neurones in rat hippocampus in vitro. *J. Physiol.*, **524 Part 1**, 91–116.

Malinow, R. & Tsien, R.W. (1990) Presynaptic enhancement shown by whole-cell recordings of long-term potentiation in hippocampal slices. *Nature*, **346**, 177–180.

McBain, C.J., DiChiara, T.J. & Kauer, J.A. (1994) Activation of metabotropic glutamate receptors differentially affects two classes of hippocampal interneurons and potentiates excitatory synaptic transmission. *J. Neurosci.*, **14**, 4433–4445.

Poncer, J.C., McKinney, R.A., Gähwiler, B.H. & Thompson, S.M. (1997) Either N- or P-type calcium channels mediate GABA release at distinct hippocampal inhibitory synapses. *Neuron*, **18**, 463–472.

Pouille, F. & Scanziani, M. (2001) Enforcement of temporal fidelity in pyramidal cells by somatic feed-forward inhibition. *Science*, **293**, 1159–1163.

Pouille, F. & Scanziani, M. (2004) Routing of spike series by dynamic circuits in the hippocampus. *Nature*, **429**, 717–723.

Price, C.J., Cauli, B., Kovacs, E.R., Kulik, A., Lambolez, B., Shigemoto, R. & Capogna, M. (2005) Neurogliaform neurons form a novel inhibitory network in the hippocampal CA1 area. *J. Neurosci.*, **25**, 6775–6786.

Remondes, M. & Schuman, E.M. (2002) Direct cortical input modulates plasticity and spiking in CA1 pyramidal neurons. *Nature*, **416**, 736–740.

Sik, A., Penttonen, M. & Buzsaki, G. (1997) Interneurons in the hippocampal dentate gyrus: an in vivo intracellular study. *Eur. J. Neurosci.*, **9**, 573–588.

Somogyi, P. & Klausberger, T. (2005) Defined types of cortical interneurone structure space and spike timing in the hippocampus. *J. Physiol.*, **562**, 9–26.

Stoppini, L., Buchs, P.A. & Muller, D. (1991) A simple method for organotypic cultures of nervous tissue. *J. Neurosci. Meth.*, **37**, 173–182.

Thomas, A.M., Corona-Morales, A.A., Ferraguti, F. & Capogna, M. (2005) Sprouting of mossy fibers and presynaptic inhibition by group II metabotropic glutamate receptors in pilocarpine-treated rat hippocampal slice cultures. *Neuroscience*, **131**, 303–320.

Vida, I., Halasy, K., Szinyei, C., Somogyi, P. & Buhl, E.H. (1998) Unitary IPSPs evoked by interneurons at the stratum radiatum-stratum lacunosum-moleculare border in the CA1 area of the rat hippocampus in vitro. *J. Physiol.*, **506**, 755–773.

Williams, S. & Lacaille, J.C. (1992) GABAB receptor-mediated inhibitory postsynaptic potentials evoked by electrical stimulation and by glutamate stimulation of interneurons in stratum lacunosum-moleculare in hippocampal CA1 pyramidal cells in vitro. *Synapse*, **11**, 249–258.

Williams, S., Samulack, D.D., Beaulieu, C. & LaCaille, J.C. (1994) Membrane properties and synaptic responses of interneurons located near the stratum lacunosum-moleculare/radiatum border of area CA1 in whole-cell recordings from rat hippocampal slices. *J. Neurophysiol.*, **71**, 2217–2235.

Witter, M.P. (1993) Organization of the entorhinal-hippocampal system: a review of current anatomical data. *Hippocampus*, **3 Spec No**, 33–44.

Witter, M.P., Griffioen, A.W., Jorritsma-Byham, B. & Krijnen, J.L. (1988) Entorhinal projections to the hippocampal CA1 region in the rat: an underestimated pathway. *Neurosci. Lett.*, **85**, 193–198.

Yeckel, M.F. & Berger, T.W. (1990) Feedforward excitation of the hippocampus by afferents from the entorhinal cortex: redefinition of the role of the trisynaptic pathway. *Proc. Natl Acad. Sci. USA*, **87**, 5832–5836.

Yeckel, M.F. & Berger, T.W. (1995) Monosynaptic excitation of hippocampal CA1 pyramidal cells by afferents from the entorhinal cortex. *Hippocampus*, **5**, 108–114.

Zimmer, J. & Gähwiler, B.H. (1984) Cellular and connective organization of slice cultures of the rat hippocampus and fascia dentata. *J. Comp. Neurol.*, **228**, 432–446.

Zsiros, V., Aradi, I. & Maccaferri, G. (2007) Propagation of postsynaptic currents and potentials via gap junctions in GABAergic networks of the rat hippocampus. *J. Physiol.*, **578**, 527–544.

Zsiros, V. & Maccaferri, G. (2005) Electrical coupling between interneurons with different excitable properties in the stratum lacunosum-moleculare of the juvenile CA1 rat hippocampus. *J. Neurosci.*, **25**, 8686–8695.